Mathematical Biosciences xxx (2008) xxx–xxx

Contents lists available at ScienceDirect

Mathematical Biosciences

journal homepage: www.elsevier.com/locate/mbs

Model-based identification and diagnosis of a porcine model of induced endotoxic shock with hemofiltration

C. Starfinger [a,*], J.G. Chase [a], C.E. Hann [a], G.M. Shaw [b], B. Lambermont [c], A. Ghuysen [c], P. Kolh [c], P.C. Dauby [d], T. Desaive [d]

[a] Centre for Bioengineering, University of Canterbury, Private Bag 4800, Christchurch, New Zealand
[b] Department of Intensive Care Medicine, Christchurch Hospital, Christchurch, New Zealand
[c] Hemodynamics Research Laboratory, University of Liège, Belgium
[d] Institute of Physics, University of Liège, Belgium

ARTICLE INFO

Article history:
Received 27 January 2008
Received in revised form 15 June 2008
Accepted 21 August 2008
Available online xxxx

Keywords:
Cardiovascular system
Cardiac model
Parameter identification
Integral method
Endotoxin
Hemofiltration
Septic shock

ABSTRACT

A previously validated cardiovascular system (CVS) model and parameter identification method for cardiac and circulatory disease states are extended and further validated in a porcine model ($N = 6$) of induced endotoxic shock with hemofiltration. Errors for the identified model are within 10% when the model is re-simulated and compared to the clinical data. All identified parameter trends over time in the experiments match clinically expected changes both individually and over the cohort. This work represents a further clinical validation of these model-based cardiovascular diagnosis and therapy guidance methods for use with monitoring endotoxic disease states.

1. Introduction

Sepsis is a very complex and serious systemic response to infection that also has a significant impact on cardiovascular and circulatory performance. Sepsis results in as many deaths in the USA as out-of-hospital cardiac arrests, and four times the number for breast cancer [1]. More specifically, mortality rates have ranged from 25% to 80% over the last few decades [2]. Septic shock or severe sepsis and multiple organ failure are thus one of the leading causes for morbidity and mortality in the critical care setting. Since continuous hemofiltration (HF) was first described as a new form of renal replacement therapy [3], a lot of experimental research has shown that hemofiltration can also improve hemodynamics and survival in septic shock.

This research identifies parameters using a previously described cardiovascular system (CVS) model and parameter identification process [4–7], using data from a porcine experiment of induced endotoxic shock, combined with continuous veno-venous hemofiltration (CVVH) [8]. Measurements used to identify the model parameters are the: minimum and maximum volumes in the ventricles (V_{lv}, V_{rv}), pressures in aorta, pulmonary artery (P_{ao}, P_{pa}) and heart rate (HR). All of these are reasonably measured or estimated in a critical care setting. Every 30 min into the experiment new parameters are identified that uniquely represent the pig's hemodynamic condition at that time. It is shown that the model is able to accurately capture all the pressures and volumes when compared to measured clinical data. Every 30 min into the experiment new parameters are identified that uniquely represent the pig's hemodynamic condition at that time. It is shown that the model is able to accurately capture all the pressures and volumes when compared to measured clinical data.

In contrast to other research groups, which mainly use Windkessel models to determine small parts of the circulation (such as the right ventricular afterload) [9], the CVS model presented in this research simulates the full circulation. This full representation of the circulatory system allows the identification of all main physiologically important parameters. For example, the two vascular resistances R_{sys} and R_{pulin}, as well as the resistances to venous return (R_{vr} and R_{pulout}) are available and can be tracked during the development of septic shock.

The main goal of this research is thus twofold. Firstly, the previously presented CVS model is further validated – in this research for septic shock data. This shows the overall validity and applicability of the model and methods developed. Secondly, this research shows a first practical approach for assessing the best therapy in

* Corresponding author.
E-mail address: cst45@student.canterbury.ac.nz (C. Starfinger).

0025-5564/$ - see front matter © 2008 Elsevier Inc. All rights reserved.
doi:10.1016/j.mbs.2008.08.014

sepsis. The model parameters can be used to track the developing septic condition. For example, tracking systemic vascular resistance (R_{sys}) in real-time could be an extremely useful tool for a practitioner. As a result, therapeutic decisions can be optimally guided. More specifically, as R_{sys} drops an optimized dose of vasopressors (as opposed to inotropic drugs) can be determined and prescribed.

2. Methodology

2.1. CVS model

The CVS model used in this research is a lumped parameter model previously developed in [10,11], and based on earlier models [12,13]. The original model consists of six elastic chambers, with two chambers for the left and right ventricle, respectively, and has been used in identifying/diagnosing Pulmonary Embolism [5]. These pressure–volume chambers are each characterized by the flow in and out of the chamber, the pressure up- and downstream, the resistances of the heart valves, and inertia of the blood – as given for the left ventricle (LV) by the following equations:

$$V_{lv} = V_{lvf} + V_{spt}, \tag{1}$$
$$V_{pcd} = V_{lv} + V_{rv}, \tag{2}$$
$$P_{pcd} = P_{0pcd} \cdot \left(e^{\lambda_{pcd}\left(V_{pcd} - V_{0pcd}\right)} - 1 \right), \tag{3}$$
$$P_{peri} = P_{pcd} + P_{th}, \tag{4}$$
$$\dot{Q}_{av} = \frac{(P_{lv} - P_{ao} - Q_{av} \cdot R_{av})}{L_{av}}, \tag{5}$$
$$\dot{Q}_{mt} = \frac{(P_{pu} - P_{lv} - Q_{mt} \cdot R_{mt})}{L_{mt}}, \tag{6}$$
$$P_{pu} = E_{pu} \cdot (V_{pu} - V_{dpu}) + P_{th}, \tag{7}$$
$$P_{ao} = E_{ao} \cdot (V_{ao} - V_{dao}), \tag{8}$$
$$P_{sys} = E_{sys} \cdot (V_{sys} - V_{dsys}), \tag{9}$$
$$P_{cap} = E_{cap} \cdot (V_{cap} - V_{cap}), \tag{10}$$
$$\dot{V}_{pv} = Q_{pulout} - Q_{mt}, \tag{11}$$
$$\dot{V}_{ao} = Q_{av} - Q_{sys}, \tag{12}$$
$$\dot{V}_{sys} = Q_{sys} - Q_{vr}, \tag{13}$$
$$\dot{V}_{cap} = Q_{pulin} - Q_{pulout}, \tag{14}$$
$$Q_{sys} = \frac{(P_{ao} - P_{sys})}{R_{sys}}, \tag{15}$$
$$Q_{vr} = \frac{(P_{sys} - P_{vc})}{R_{vr}}, \tag{16}$$
$$Q_{pulin} = \frac{(P_{pa} - P_{cap})}{R_{pulin}}, \tag{17}$$
$$Q_{pulout} = \frac{(P_{cap} - P_{pu})}{R_{pulout}}, \tag{18}$$
$$P_{lv} = P_{lvf} + P_{peri}, \tag{19}$$
$$P_{spt} = \text{driS} \cdot E_{esspt}(V_{spt} - V_{dspt}) \tag{20}$$
$$+ (1 - \text{driS}) \cdot P_{0spt}\left(e^{\lambda_{spt}\left(V_{spt} - V_{ospt}\right)} - 1 \right), \tag{21}$$

where all abbreviations are explained in Table 2, as also shown in Fig. 1. Similar equations are obtained for the right ventricle (RV).

The original model [10,11] has been extended previously [6,7] and an overview of the extended model is given in Fig. 1. The extended CVS model adds two new compartments $(P,V)_{sys}$ and $(P,V)_{cap}$, which represent the systemic and pulmonary capillaries, respectively. Furthermore, two new resistances, the resistance to venous return (R_{vr}) and the outflow pulmonary resistance (R_{pulout}) were added.

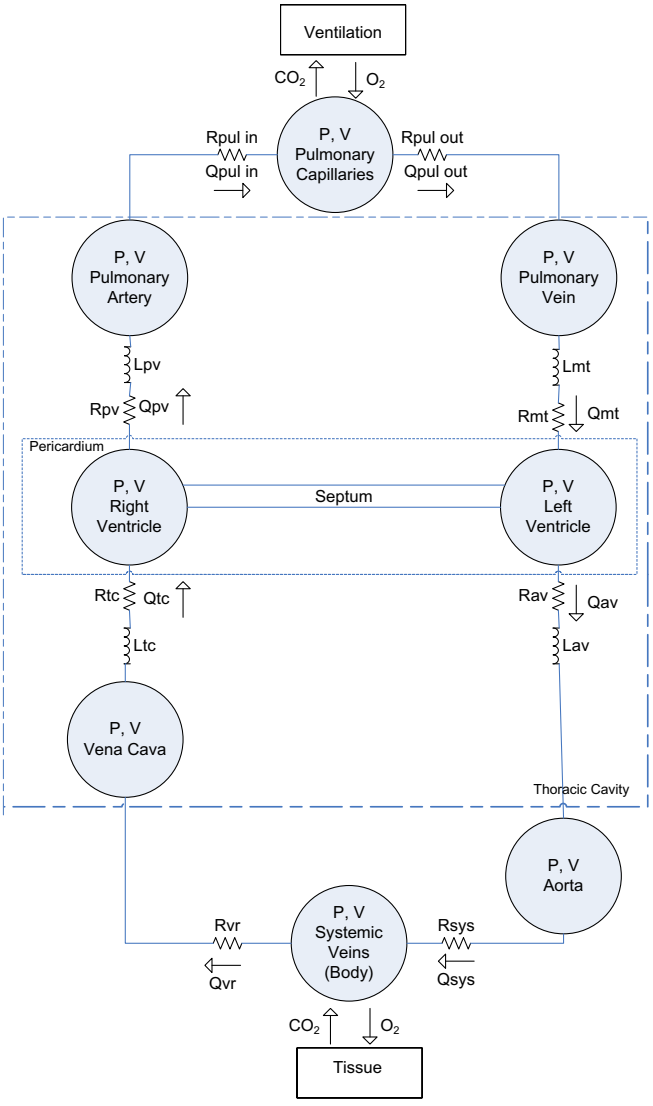

Fig. 1. Extended CVS model overview which includes additional compartments $(P,V)_{sys}$ and $(P,V)_{cap}$ to differentiate the arterial and venous sides of the pulmonary and systemic circulation.

These modifications are required to allow a more realistic and physiologically relevant representation of the physiological behavior encountered during mechanical or spontaneous breathing [7,14]. The vena cava is now also part of the thoracic cavity, although the aorta and pulmonary capillaries are not included. This structure is a more physiologically and anatomically accurate representation with the pulmonary arteries and veins, as well as the vena cava, located in the thoracic cavity. However, neither the aorta (as modelled as part of the systemic circulation) nor the lung capillaries (which are surrounded by alveolar pressure) are subjected by intrathoracic pressure (P_{th}). More details about the new model definition are available in [6,7].

2.2. Integral-based parameter identification

The parameter identification method used in this research has been shown to rapidly and accurately identify almost the entire parameter set in the presence of significant measurement noise [4–6]. This research uses an adjusted identification method and process for the revised model, as previously presented [6,7] and

Table 1
Parameters used in CVS model

Taken from the literature or measured
P_{th}, period, λ_{lvf}, λ_{rvf}, λ_{spt}, λ_{pcd}, E_{esspt}, Vd_{spt}, Vo_{spt}, Po_{spt}, Vo_{lvf}, Vo_{rvf}, Vd_{lvf}, Vd_{rvf}, Vd_{vc}, Vd_{ao}, Vd_{pa}, Vd_{pv}
Optimized
L_{av}, L_{mt}, L_{tc}, L_{pv}, E_{eslvf}, P_{0lvf}, E_{esrvf}, P_{0rvf}, R_{av}, R_{mt}, R_{tc}, R_{pv}, P_{ao0}, P_{pu0}, P_{pa0}, P_{vc0}, P_{0pcd}, E_{sys}, E_{cap}, E_{ao}, E_{pa}, E_{vc}, E_{pu}, R_{sys}, R_{pulin}, R_{pulout}, R_{vr}

summarized hereafter. Table 1 lists all the model variables and states that must be either measured, estimated or identified from measured data. Consider the CVS model where, for example V_{ao} is given by:

$$V_{ao}(t) - V_{ao0} = \int_0^t (Q_{av} - Q_{sys})\,dt. \tag{22}$$

Using Eq. (22), the equation defining the pressure in the aorta, P_{ao}, can be rewritten as:

$$P_{ao}(t) = P_{ao0} + E_{ao} \cdot \int_0^t (Q_{av} - Q_{sys})\,dt, \tag{23}$$

which after substituting the equation for Q_{sys} into Eq. (23) and reordering yields the following matrix for determining the parameter E_{ao}:

$$\begin{pmatrix} \int Q_{av} & \int P_{ao} & \int P_{sys} \end{pmatrix} \cdot \begin{pmatrix} E_{ao} \\ A_1 \\ A_2 \end{pmatrix} = \begin{pmatrix} P_{ao} - P_{ao0} \end{pmatrix}, \tag{24}$$

with $A_1 = \frac{-E_{ao}}{R_{sys}}$ and $A_2 = \frac{E_{ao}}{R_{sys}}$. Similarly, the following matrices are obtained for E_{pa}, E_{vc}, E_{pu}, E_{cap}, E_{sys}, R_{sys}, R_{pulin}, R_{vr} and R_{pulout}. Note, that for reasons of simplicity and clarity, the differential dt and the upper and lower limits of the integration symbol $\int$ are omitted. Usually and if not stated otherwise, the integration is done over one heart beat. In cases where matrices are constructed separately for ejection and filling periods, the integrals are only calculated during these periods.

$$\begin{pmatrix} \int Q_{pv} & \int P_{pa} & \int P_{cap} \end{pmatrix} \cdot \begin{pmatrix} E_{pa} \\ A_3 \\ A_4 \end{pmatrix} = \begin{pmatrix} P_{pa} - P_{pa0} \end{pmatrix}, \tag{25}$$

with $A_3 = \frac{-E_{pa}}{R_{pulin}}$ and $A_4 = \frac{E_{pa}}{R_{pulin}}$.

$$\begin{pmatrix} \int Q_{av} & \int V_{sys,eff} & P_{ao} - P_{ao0} \end{pmatrix} \cdot \begin{pmatrix} R_{sys} \\ E_{sys} \\ A_5 \end{pmatrix} = \begin{pmatrix} \int P_{ao} \end{pmatrix}, \tag{26}$$

with $A_5 = \frac{-R_{sys}}{E_{ao}}$.

$$\begin{pmatrix} \int Q_{pv} & \int V_{cap,eff} & P_{pa} - P_{pa0} \end{pmatrix} \cdot \begin{pmatrix} R_{pulin} \\ E_{cap} \\ A_6 \end{pmatrix} = \begin{pmatrix} \int P_{pa} \end{pmatrix}, \tag{27}$$

with $A_6 = \frac{-R_{pulin}}{E_{pa}}$.

$$\begin{pmatrix} \int Q_{tc} & \int V_{vc} & P_{vc} - P_{vc0} \end{pmatrix} \cdot \begin{pmatrix} R_{vr} \\ E_{vc} \\ A_7 \end{pmatrix} = \begin{pmatrix} \int P_{sys} - \int P_{th} \end{pmatrix}, \tag{28}$$

with $A_7 = \frac{R_{vr}}{E_{vc}}$.

$$\begin{pmatrix} \int Q_{mt} & \int V_{pv} & P_{pu} - P_{pu0} \end{pmatrix} \cdot \begin{pmatrix} R_{pulout} \\ E_{pu} \\ A_8 \end{pmatrix} = \begin{pmatrix} \int P_{cap} - \int P_{th} \end{pmatrix}, \tag{29}$$

with $A_8 = \frac{R_{pulout}}{E_{pu}}$.

2.2.1. Extended integral-based identification

The main adjustments to the identification method, originally presented in [4], include keeping the elastances (E_{ao}, E_{pa}) fixed at estimated values, thus allowing other parameters to be more easily and accurately identified. The elastances E_{ao} and E_{pa} in the CVS model are now estimated (assuming zero unstressed volumes V_{dao} and V_{dpa}) [6]:

$$E_{ao} = 1.25 \cdot \frac{PP_{ao}}{SV}, \tag{30}$$

$$E_{pa} = 1.25 \cdot \frac{PP_{pa}}{SV}, \tag{31}$$

where PP_{ao} and PP_{pa} are the measured arterial and pulmonary artery pulse pressures and SV is the stroke volume. Importantly, the effect of a slightly over- or underestimated value for E_{ao} and E_{pa} will cancel as the trends over time of these elastances are what is clinically important, rather than their absolute values. Furthermore, as E_{ao} is given, Eq. (26) can now directly be solved for R_{sys} and E_{sys}:

$$R_{sys} = \frac{E_{ao} \cdot (\int P_{sys} - \int P_{ao})}{(P_{ao} - P_{ao0} - \int Q_{av} \cdot E_{ao})}, \tag{32}$$

$$E_{sys} = \frac{\int P_{ao} - R_{sys} \cdot (\int Q_{av} - 1/E_{ao} \cdot (P_{ao} - P_{ao0}))}{\int V_{sys,eff}}. \tag{33}$$

Similarly, Eq. (27) can be solved for R_{pulin} and E_{cap}:

$$R_{pulin} = \frac{E_{pa} \cdot (\int P_{cap} - \int P_{pa})}{(P_{pa} - P_{pa0} - \int Q_{pv} \cdot E_{pa})}, \tag{34}$$

$$E_{cap} = \frac{\int P_{pa} - R_{pulin} \cdot (\int Q_{pv} - 1/E_{pa} \cdot (P_{pa} - P_{pa0}))}{\int V_{cap,eff}}. \tag{35}$$

Using Eqs. (32)–(34) simplifies the parameter identification process as now less parameters have to be identified, but are directly given (estimated) or easily calculated. Thus, the identifiability of the parameter set is guaranteed and the identified parameters are more reliable and robust and found in a consistent way.

The remaining parameters given in Table 1 are identified based on the previously published integral-based identification process [4,5]. Briefly, the following system of linear equations can be defined:

$$\mathbf{A} \cdot \vec{x} = \vec{b}, \tag{36}$$

$$\vec{x} = \begin{pmatrix} L_{av}, & L_{mt}, & L_{tc}, & L_{pv}, & E_{eslvf}, & P_{0lvf}, & E_{esrvf}, & P_{0rvf}, \\ R_{av}, & R_{mt}, & R_{tc}, & R_{pv}, & ~~P_{ao0},~~ & ~~P_{pu0},~~ & ~~P_{pa0},~~ & P_{vc0} \end{pmatrix}^{\top}, \tag{37}$$

where $\mathbf{A}$ is an $N \times$ ~~18~~ matrix, N is the number of integration periods over which the parameters are constant, $\vec{b}$ is an $N \times 1$ vector, $\vec{x}$ are the patient specific parameters ~~and the initial conditions, P_{ao0}, P_{pu0}, P_{pa0} and P_{vc0} are treated as extra unknown variables.~~ Eq. (36) can then be solved by linear least squares to uniquely determine $\vec{x}$.

Constraints can be added, if desired, and matrix $\mathbf{A}$ and vector $\vec{b}$ are defined for the ejection ('eject') and filling ('fill') periods of the cardiac cycle:

$$\mathbf{A} = \begin{pmatrix} \mathbf{A}_{lv,eject} \\ \mathbf{A}_{lv,fill} \\ \mathbf{A}_{rv,eject} \\ \mathbf{A}_{rv,fill} \end{pmatrix}, \tag{38}$$

$$\vec{b} = \begin{pmatrix} \vec{b}_{lv,eject} \\ \vec{b}_{lv,fill} \\ \vec{b}_{rv,eject} \\ \vec{b}_{rv,fill} \end{pmatrix}, \tag{39}$$

and the matrix for the left ventricle during ejection, $\mathbf{A}_{lv,eject}$, is given by:

$$\mathbf{A}_{\mathrm{lv,eject}} = \left(Q_{\mathrm{av}}(\mathrm{eb}:\mathrm{ef}) \quad \vec{0} \quad \vec{0} \quad \vec{0} \quad -Ie_1 \quad -Ie_2 \quad \vec{0} \quad \vec{0} \quad \frac{}{} V_{\mathrm{lv}}(\mathrm{eb}:\mathrm{ef}) - V_{\mathrm{lv}}(\mathrm{eb}) \quad \vec{0} \quad \vec{0} \quad \vec{0} \quad -Ie_5 \right), \tag{40}$$

where eb = ejection start and ef = ejection end for the LV. Ie_1, Ie_2 and Ie_5 are defined:

$$Ie_1 = \int_{\mathrm{eb}}^{\mathrm{ef}} (V_{\mathrm{lvf}} - V_{\mathrm{dlvf}}) \cdot \mathrm{driL}, \tag{41}$$

$$Ie_2 = \int_{\mathrm{eb}}^{\mathrm{ef}} (1 - \mathrm{driL}) \cdot \left(e^{(\lambda_{\mathrm{lvf}} \cdot (V_{\mathrm{lvf}} - V_{\mathrm{olvf}}))} - 1 \right), \tag{42}$$

$$Ie_5 = \int_{\mathrm{eb}}^{\mathrm{ef}} \left(e^{(\lambda_{\mathrm{pcd}} \cdot (V_{\mathrm{lv}} + V_{\mathrm{rv}} - V_{\mathrm{opcd}}))} - 1 \right). \tag{43}$$

The matrix for the left ventricle during filling, $\mathbf{A}_{\mathrm{lv,fill}}$, is given by:

$$\mathbf{A}_{\mathrm{lv,fill}} = \left(\vec{0} \quad Q_{\mathrm{mt}}(\mathrm{fb}:\mathrm{ff}) \quad \vec{0} \quad \vec{0} \quad If_1 \quad If_2 \quad \vec{0} \quad \vec{0} \quad \vec{0} \quad V_{\mathrm{lv}}(\mathrm{fb}:\mathrm{ff}) - V_{\mathrm{lv}}(\mathrm{fb}) \quad \vec{0} \quad \vec{0} \quad If_5 \right), \tag{44}$$

where fb = filling start and ff = filling end for the LV. If_1, If_2 and If_5 are defined as:

$$If_1 = \int_{\mathrm{fb}}^{\mathrm{ff}} (V_{\mathrm{lvf}} - V_{\mathrm{dlvf}}) \cdot \mathrm{driL}, \tag{45}$$

$$If_2 = \int_{\mathrm{fb}}^{\mathrm{ff}} (1 - \mathrm{driL}) \cdot \left(e^{(\lambda_{\mathrm{lvf}} \cdot (V_{\mathrm{lvf}} - V_{\mathrm{olvf}}))} - 1 \right), \tag{46}$$

$$If_5 = \int_{\mathrm{fb}}^{\mathrm{ff}} \left(-e^{(\lambda_{\mathrm{pcd}} \cdot (V_{\mathrm{lv}} + V_{\mathrm{rv}} - V_{\mathrm{opcd}}))} - 1 \right). \tag{47}$$

Vector $\vec{b}_{\mathrm{lv,eject}}$ for the left ventricle during ejection is given by:

$$\vec{b}_{\mathrm{lv,eject}} = P_{\mathrm{th}} \cdot (t(\mathrm{eb}:\mathrm{ef}) - t(\mathrm{eb})) - \int P_{\mathrm{ao}}. \tag{48}$$

Vector $\vec{b}_{\mathrm{lv,fill}}$ for the left ventricle during filling is given by:

$$\vec{b}_{\mathrm{lv,fill}} = \int P_{\mathrm{pu}} - P_{\mathrm{th}} \cdot (t(\mathrm{fb}:\mathrm{ff}) - t(\mathrm{fb})). \tag{49}$$

Similar equations are obtained for the right ventricle during filling and ejection. More detailed information about the derivation and computation of these terms of the identification process can be found in [4,5].

2.2.2. Scaling process

Given only discrete measurements of peak and minimum values, the waveforms are not known and the original integral method of [4] cannot be directly applied. However, waveforms can be approximately generated by scaling a set of previously calculated model outputs to best fit the maximum and minimum data values measured for the pressures and volumes. The assumption is that these validated model waveforms are reasonably conformable with the actual clinical case. In addition, because they capture the maximum and minimum measured values, they also enable the best fit that the given model can provide.

These scaled signals are then re-identified using these approximated waveforms and a new CVS forward simulation is performed with the previously identified parameters to produce a much closer match to the clinical data than the first initial parameter set. This simulated output is then compared to the clinical data to assess performance. Subsequently, the output signals are re-scaled and new parameters are identified, which are then again used to run another simulation. This iterative process is stopped when the relative error between model output and clinical data reaches a set tolerance or fails to improve. Fig. 2 gives an overview of this overall identification process, where the major change from [4] is the iterative process using scaled, approximate waveforms in place of difficult to measure clinical waveforms.

2.2.3. Substitution of flow integrals during the scaling process

Another adjustment to the parameter identification process has been made to better calculate the parameters that are determined by the flows in and out of the ventricles. Previously, these flows have been used in the identification process and significant error was introduced during the waveform scaling process as a result. The flow integrals $\int Q_{\mathrm{mt}}$, $\int Q_{\mathrm{av}}$, $\int Q_{\mathrm{tc}}$ and $\int Q_{\mathrm{pv}}$ are now substituted by their corresponding volumes, as previously presented in [6]. This change has the advantage that the volumes in the ventricles are measured, or at least estimated signals where the flows themselves are not usually directly measured or estimated.

2.3. Experimental protocol and physiological measurements

All experimental procedures for this experiment were reviewed and approved by the Ethics Committee of the Medical Faculty of the University of Liège. They were performed in accordance with the *Guide for the Care and Use of Laboratory Animals*, as adopted and promulgated by the US National Institutes of Health (NIH Publication No. 85-23, revised 1996). The experiments were performed on six healthy pigs weighing 25–30 kg. All measurements for one pig and eight measurements of the remaining five pigs had to be omitted from the final analysis as they contained corrupted data, such as those produced by disconnected catheters.

The animals were premedicated and anesthetized, as described previously [9]. Measurements were obtained for systemic arterial pressure (P_{ao}), pulmonary arterial pressure (P_{pa}) and the left and right ventricle pressures and volumes (P_{lv}, V_{lv}, P_{rv}, V_{rv}) as described in [9]. In particular, volume measurements are made by a 7F, 12-electrode (8 mm interelectrode distance) conductance micromanometer-tipped catheter (CD Leycom, Zoetermeer, The Netherlands).

After a 30 min stabilization period, the animals received a 0.5 mg/kg endotoxin infusion (lipopolysaccharide from *Escherichia coli* serotype 0127:B8; Sigma Chemical, St. Louis, MO, USA) over a 30 min period (T000–T030). From 60 min (T060) into the experiment onwards, the animals underwent a zero-balance continuous veno-venous hemofiltration (CVVH) at a rate of 45 ml/kg/h. A 0.7 m^2 large-pore (78 Å) membrane with a cutoff of 80 kDa (Sureflux FH 70, Nipro, Osaka, Japan) and a Baxter BM 25–BM 14 hemo-

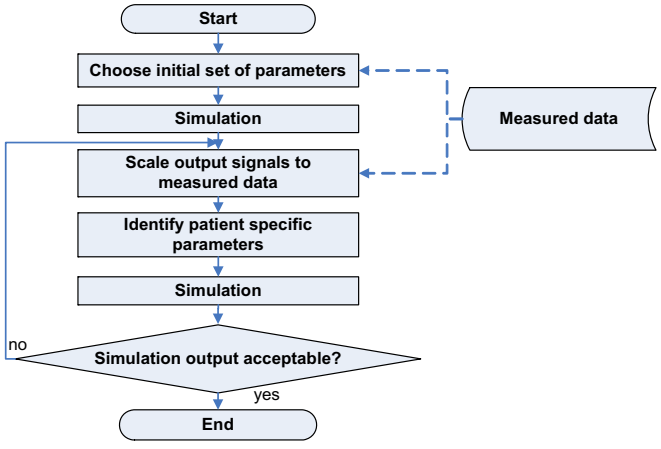

Fig. 2. Parameter identification algorithm: (1) a set of parameters is used for an initial simulation, (2) data are then scaled to match the measured data and (3) identified. This process is iterated until the simulation output is acceptable.

filtration device (Baxter Health Care, Munich, Germany) were used. Ultrafiltrate was replaced in the postdilution mode by a bicarbonate-buffered hemofiltration fluid (Na^+: 150 mM; K_+: 3 mM; bicarbonate: 30 mM) at a temperature of 37 °C.

3. Results

3.1. Identification of endotoxic shock

Fig. 3 illustrates the very good matches achieved for one typical pig in detail. The first two subfigures ((a) and (b)) show the left and right ventricle signals at the beginning of the experiment (T000). The upper panel of the left subfigure (LV) shows the clinical (V_{lvp}) vs. simulated left ventricle volume (V_{lvs}) and in the lower panel the clinical (P_{lvp}) vs. simulated left ventricle pressure (P_{lvs}) and arterial pressure (P_{aop},P_{aos}), respectively. The right subfigure (RV) illustrates the same results for the right ventricle volume (V_{rv}, upper panel) and the right ventricle pressure and pulmonary artery pressure (P_{rv}, P_{pa}, lower panel). The following four subfigures ((c)–(f)) show the same signals at 120 min into the experiment and at 240 min. In each case, the matches between pig-specific, identified model and clinical data are qualitatively very good.

Fig. 4 summarizes the results obtained for all identified times (from t000 to t240 min) over all pigs and shows the clinically measured end-diastolic (EDV) and end-systolic (ESV) left ventricle volumes (solid lines). The crosses and boxes represent the CVS model

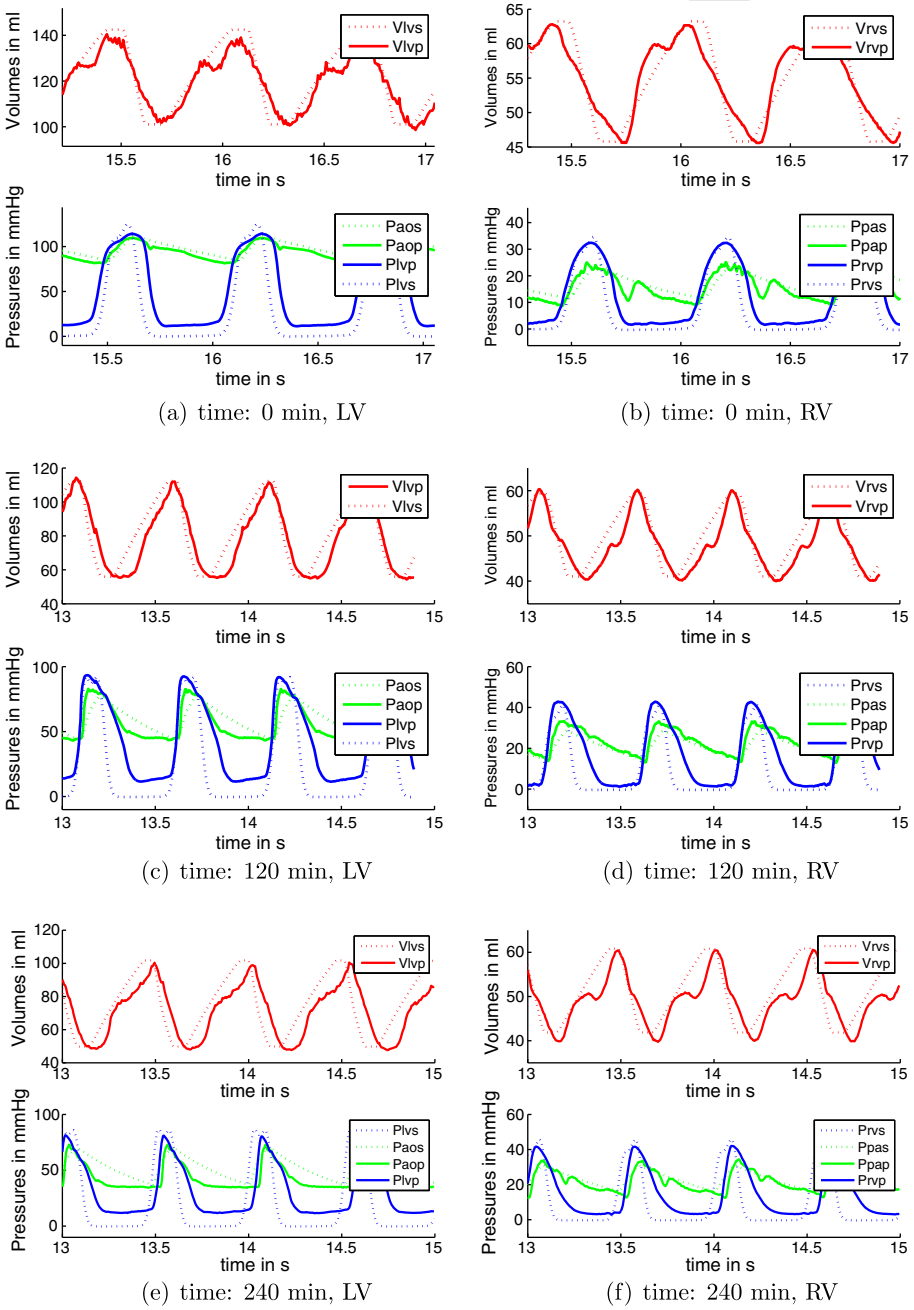

(a) time: 0 min, LV (b) time: 0 min, RV

(c) time: 120 min, LV (d) time: 120 min, RV

(e) time: 240 min, LV (f) time: 240 min, RV

Fig. 3. Model output (dotted) vs. clinical (solid line) volume and pressure signals for left and right ventricle (LV, RV). The upper panel shows the clinical (p) vs. simulated ventricle volume (s). The lower panel shows the clinical (p) vs. simulated (s) ventricle and arterial pressure. The results are shown for 0 min (begin), 120 min (middle) and 240 min (end) into the experiment. (a) Time: 0 min, LV (b) time: 0 min, RV (c) time: 120 min, LV (d) time: 120 min, RV (c) time: 240 min, LV (e) time: 240 min, RV.

Please cite this article in press as: C. Starfinger et al., Model-based identification and diagnosis of a porcine model of induced ..., Math. Biosci. (2008), doi:10.1016/j.mbs.2008.08.014

simulation output when re-run using the identified model parameters. As can be seen, the model output values match the true clinical values very well with mean absolute percentage errors less than 3%, which is well within measurement or estimate errors [15,16]. Fig. 5 shows the same results for the right ventricle volumes, respectively.

Fig. 6 shows the matched systemic arterial systolic and arterial diastolic pressure values (SAP, DAP). Solid lines represent the clinical measurements and the crosses, boxes the CVS model outputs. Again, very good matches are obtained with mean absolute percentage errors less than 7%.

Fig. 7 shows the same results for the systolic and diastolic pulmonary artery pressures (SPAP, DPAP), respectively. Note, that the match between the two signals shows larger errors for measurements 34–38, because the clinically measured P_{pa} signal went below zero, a non-physiological value that is almost certainly a measurement error rather than a true measurement. These measurements were thus ignored during the identification process, but represent the kinds of errors that can occasionally occur.

It has to be noted, that during the identification process only the systolic (maximum) and diastolic (minimum) values of the measured ventricle volume (EDV, ESV) and arterial pressure (SAP, DAP) are used. The ventricle pressures (P_{lv}, P_{rv}) are not needed in the identification as they are divided into their corresponding volumes (V_{lvf} and V_{rvf}) and driver functions as seen in Eqs. (41)–(43) and (45)–(47). However, it can clearly be seen that relatively good matches are nevertheless obtained for the ventricle pressures, further validating the model and identification process.

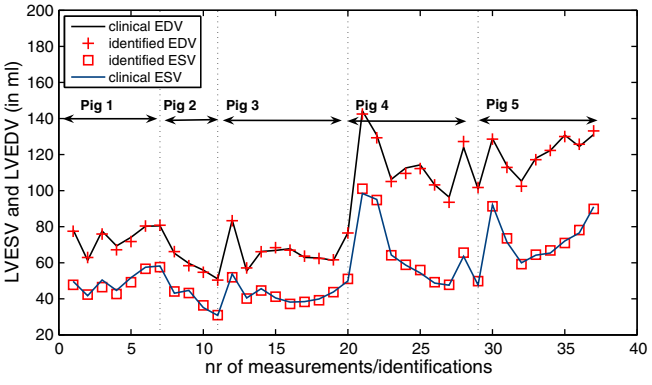

Fig. 4. Model output (+, □) vs. clinical (solid line) left ventricle volumes for all identified times (from t000 to t240 min) over all pigs. The upper line shows the clinical vs. identified (+) end-diastolic volume (LVEDV) and the lower line shows clinical vs. identified (□) end-systolic volume (LVESV).

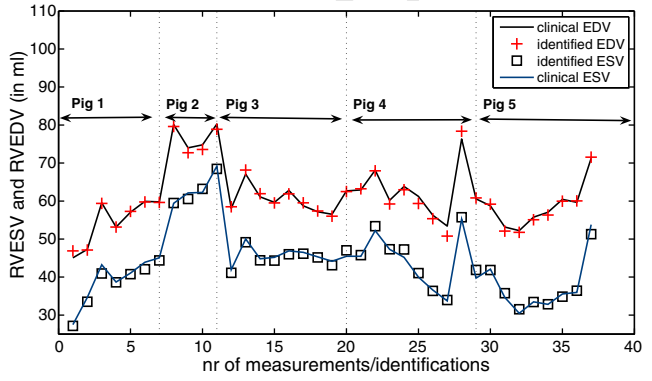

Fig. 5. Model output (+, □) vs. clinical (solid line) right ventricle volumes for all identified times (from t000 to t240 min) over all pigs. The upper line shows the clinical vs. identified (+) end-diastolic volume (RVEDV) and the lower line shows clinical vs. identified (□) end-systolic volume (RVESV).

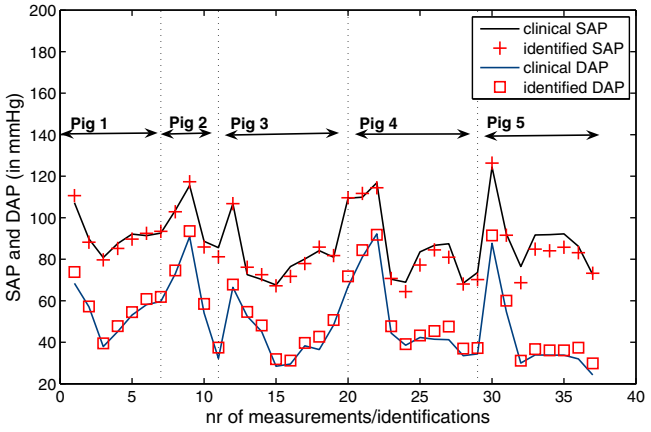

Fig. 6. Model output (+, □) vs. clinical (solid line) arterial pressure for all identified times (from t000 to t240 min) over all pigs. The upper line shows the clinical vs. identified (+) systolic arterial pressure (SAP) and the lower line shows clinical vs. identified (□) diastolic arterial pressure (DAP).

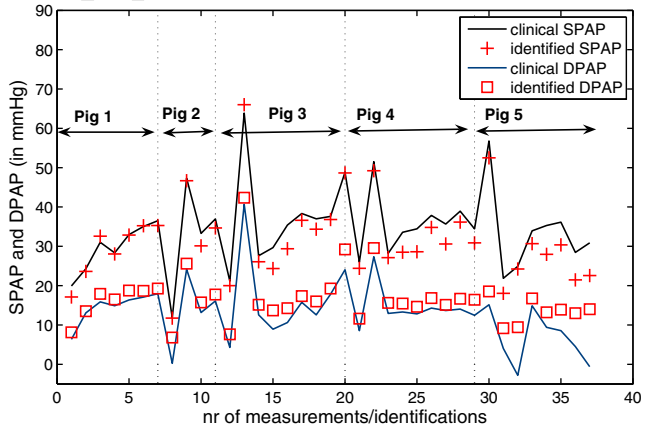

Fig. 7. Model output (+, □) vs. clinical (solid line) pulmonary artery pressure for all identified times (from t000 to t240 min) over all pigs. The upper line shows the clinical vs. identified (+) systolic pulmonary artery pressure (SPAP) and the lower line shows clinical vs. identified (□) diastolic pulmonary artery pressure (DPAP).

If desired, the ventricle pressures could easily be matched more accurately by adjusting the simple activation functions used in the CVS model [11]. However, this level of accuracy and added modification was not intended in this study and is not necessary given the good match between re-simulated model and clinical data.

Importantly, this study did not intend to accurately match the pressure and volume waveform shapes, but only the minimum (diastolic) and maximum (systolic) values. This goal was adopted because the main focus is to identify the overall macro-hemodynamic condition, and less interest is thus placed on exactly matching specific waveforms. For example, exactly matching the dicrotic notch in the arterial pressure signals was not a goal. These smaller, less clinically relevant dynamics are often a function of small unmodelled non-linearities or small non-linearities in patient-specific cardiac activation function. In addition, a patient-specific activation function would eliminate most of these clinically insignificant differences.

Table 3 shows the mean absolute percentage errors for the identified minimum and maximum pressure and volume signals (SAP, SPAP, LVESV, LVEDV, RVEDV, and RVESV) for the identified

Please cite this article in press as: C. Starfinger et al., Model-based identification and diagnosis of a porcine model of induced ..., Math. Biosci. (2008), doi:10.1016/j.mbs.2008.08.014

Table 2
Abbreviations used in the CVS model

Abbreviation	Description
λ	Parameter in EDPVR
P_0	Parameter in EDPVR
lv	Left ventricle
rv	Right ventricle
lvf	Left ventricle free wall
rvf	Right ventricle free wall
spt	Septum
pcd	Pericardium
V_0	Volume at zero pressure
V_d	Unstressed chamber volume
R	Resistance
E	Elastance
L	Inertance
P	Pressure
Q	Flow
V	Volume
mt	Mitral valve
tc	Tricuspid valve
av	Aortic valve
pv	Pulmonary valve
pulin	Systemic pulmonary
pulout	Venous pulmonary
sys	Systemic
cap	Capillary
vr	Venous return
es	End-systolic
P_{ao0}	Initial pressure ($P_{ao}(0)$) in arta
P_{pa0}	Initial pressure ($P_{pa}(0)$) in pulmonary artery
P_{vc0}	Initial pressure ($P_{vc}(0)$) in vena cava
P_{pu0}	Initial pressure ($P_{pu}(0)$) in pulmonary vein
P_{th}	Intrathoracic pressure
period	Heartbeat period
driL	Activation (driver) function for LV
driR	Activation (driver) function for RV
driS	Activation (driver) function for septum

re-simulated model over all pigs. Generally, the errors are well below 10%, which is within measurement noise. However, as mentioned before, there are a few larger errors for the pulmonary artery pressure P_{pa}, as seen in Fig. 6, that are caused by a suspiciously low non-physiological pressure signal that was ignored.

Fig. 8 shows the mean identified systemic vascular resistance (R_{sys}) over all pigs during the endotoxic shock experiment. This value is clinically important due to impact of sepsis on blood pressure, where increasing sepsis and septic shock decrease blood pressure via loss of control over systemic vascular tome and reduced resistance. This loss of resistance is clearly evident in Fig. 8 as the endotoxin experiment proceeds.

4. Discussion

The major findings of this research are twofold. Firstly, the clinical experimental results obtained previously [8] are matched using the extended CVS model and parameter identification process. Secondly, the CVS model and identification process are also

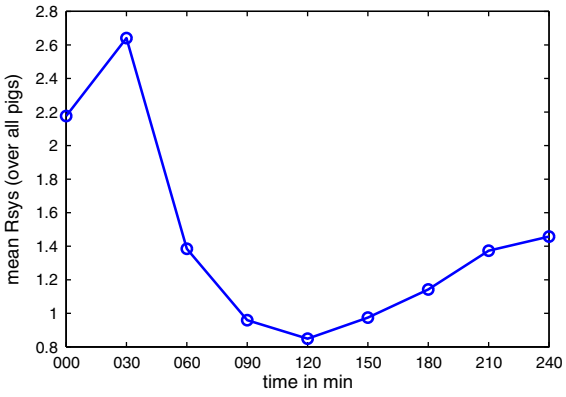

Fig. 8. Mean identified systemic vascular resistance (R_{sys}) for all five analyzed pigs during the endotoxic shock experiment. This value is clinically important due to impact of sepsis on blood pressure, where increasing sepsis and septic shock decrease blood pressure via loss of control over systemic vascular tome and reduced resistance.

further validated by correctly identifying trends observed during clinical endotoxic shock experiments [17,8,9,18–21]. Additionally, clinically significant changes in systemic vascular resistance (R_{sys}) are identified during the experiment, as shown in Fig. 8. These results match physiological expectations as low peripheral vascular resistance are a common sign in sepsis and decreases left ventricular afterload, as also seen in Fig. 6 in reduced arterial pressures. Clinically, the real time identification and tracking of R_{sys} would enable accurate determination of when to begin vasopressor therapy. In addition, based on response to an initial dose, the vasopressor dose could also be optimally titrated.

Table 3 summarizes all results for all five pigs and a total of 38 identification periods. Note, that all measurements for one pig and eight measurements of the remaining five pigs had to be omitted from this final analysis as they contained corrupted data, such as those produced by disconnected catheters. These results show that the extended CVS model is able to capture the essential dynamics of the porcine CVS response to endotoxic shock and CVVH over a selection of subjects.

Clinically, these results hold great potential significance. For critical care monitoring, important clinical indications, such as the systemic resistance (R_{sys}) can be tracked in real-time. As a result, therapeutic decisions can be optimally guided. More specifically, as R_{sys} drops an optimized dose of vasopressors (as opposed to inotropic drugs) can be determined and prescribed.

5. Conclusion

The integral-based optimization successfully identified pig-specific parameters for the extended CVS model. This further validation shows the ability of the model to adequately and realistically capture the impact of pressure–volume changes during endotoxic shock and with CVVH. In particular, the model is able

Table 3
Mean absolute percentage error (μ), standard deviation (σ) and inter-quartile range (IQR) in % for measured and simulated pressures and volumes over all identified times and pigs

	SAP	SPAP	LVEDV	LVESV	RVEDV	RVESV
Difference in % for measured and simulated pressures and volumes						
μ	3.19	7.01	1.36	2.12	1.18	1.90
σ	2.70	5.27	1.00	1.62	1.07	1.53
IQR	3.93	4.54	1.64	2.10	1.19	1.97

Abbreviations: SAP, systolic arterial pressure; SPAP, systolic pulmonary artery pressure; LVEDV, left ventricle end-diastolic volume; LVESV, left ventricle end-systolic volume; RVEDV, right ventricle end-diastolic volume; and RVESV, right ventricle end-systolic volume.

Please cite this article in press as: C. Starfinger et al., Model-based identification and diagnosis of a porcine model of induced ..., Math. Biosci. (2008), doi:10.1016/j.mbs.2008.08.014

to aggregate diverse measured data into a clear, clinically and physiologically relevant diagnostic picture as the condition develops.

More specifically, sepsis is a disease with unique whole body effects that are often counter-intuitive and in violation of the normal auto-regulatory actions of the body that it disrupts. As a result, it represents the most serious and unique challenge to any identification method for diagnosis. Hence, this research is the culmination of the series of previous works [5–7] and represents a final method in both minimal sensor data and maximum difficulty.

As discussed, the results thus offer patient-specific monitoring of otherwise unmeasurable, but clinically very significant, physiological parameters that can lead to improved therapy of care. This research thus increases confidence in the clinical applicability and validity of this overall diagnostic monitoring approach preparatory to initial studies with human subjects.

References

[1] D.C. Angus, M.A. Crowther, Unraveling severe sepsis: why did optimist fail and what's next?, JAMA 290 (2) (2003) 256
[2] D.C. Angus, W.T. Linde-Zwirble, J. Lidicker, G. Clermont, J. Carcillo, M.R. Pinsky, Epidemiology of severe sepsis in the united states: analysis of incidence, outcome, and associated costs of care, Crit. Care Med. 29 (7) (2001) 1303.
[3] P. Kramer, W. Wigger, J. Rieger, D. Matthaei, F. Scheler, Arteriovenous haemofiltration: a new and simple method for treatment of over-hydrated patients resistant to diuretics, Klin. Wochenschr. 55 (22) (1977) 1121.
[4] C.E. Hann, J.G. Chase, G.M. Shaw, Integral-based identification of patient specific parameters for a minimal cardiac model, Comput. Methods Programs Biomed. 81 (2) (2006) 181.
[5] C. Starfinger, C.E. Hann, J.G. Chase, T. Desaive, A. Ghuysen, G.M. Shaw, Model-based cardiac diagnosis of pulmonary embolism, Comput. Methods Programs Biomed. 87 (1) (2007) 46.
[6] C. Starfinger, J.G. Chase, C.E. Hann, G.M. Shaw, P. Lambert, B.W. Smith, E. Sloth, A. Larsson, S. Andreassen, S. Rees, Model-based identification of peep titrations during different volemic levels, Comput. Methods Programs Biomed 91 (2) (2008) 135.
[7] C. Starfinger, J.G. Chase, C.E. Hann, G.M. Shaw, P. Lambert, B.W. Smith, E. Sloth, A. Larsson, S. Andreassen, S. Rees, Prediction of hemodynamic changes towards peep titrations at different volemic levels using a minimal cardiovascular model, Comput. Methods Programs Biomed. 91 (2) (2008) 128.
[8] B. Lambermont, P. Delanaye, J.-M. Dogn, A. Ghuysen, N. Janssen, B. Dubois, T. Desaive, P. Kolh, V. D'Orio, J.-M. Krzesinski, Large-pore membrane hemofiltration increases cytokine clearance and improves right ventricular-vascular coupling during endotoxic shock in pigs, Artif. Organs 30 (7) (2006) 560.
[9] B. Lambermont, A. Ghuysen, P. Kolh, V. Tchana-Sato, P. Segers, P. Grard, P. Morimont, D. Magis, J.-M. Dogn, B. Masereel, V. D'Orio, Effects of endotoxic shock on right ventricular systolic function and mechanical efficiency, Cardiovasc. Res. 59 (2) (2003) 412.
[10] B.W. Smith, Minimal haemodynamic modelling of the heart and circulation for clinical application, Ph.D. Thesis, University of Canterbury, 2004.
[11] B.W. Smith, J.G. Chase, R.I. Nokes, G.M. Shaw, G. Wake, Minimal haemodynamic system model including ventricular interaction and valve dynamics, Med. Eng. Phys. 26 (2) (2004) 131.
[12] D.C. Chung, S.C. Niranjan, J.W. Clark JR, A. Bidani, W.E. Johnston, J.B. Zwischenberger, D.L. Traber, A dynamic model of ventricular interaction and pericardial influence, Am. J. Physiol. 272 (6 Pt. 2) (1997) H2942.
[13] J.B. Olansen, J.W. Clark, D. Khoury, F. Ghorbel, A. Bidani, A closed-loop model of the canine cardiovascular system that includes ventricular interaction, Comput. Biomed. Res. 33 (2000) 260.
[14] T. Desaive, B. Lambermont, A. Ghuysen, P. Kolh, P.C. Dauby, C. Starfinger, C.E. Hann, J.G. Chase, G.M. Shaw, Cardiovascular modelling and identification in septic shock – experimental validation, in: Proceedings of the 17th IFAC World Congress July 6–11, 2008, Seoul, Korea, 2008.
[15] J. Baan, E.T. van der Velde, H. de Bruin, G.J. Smeenk, J. Koops, A.D. van Dijk, D. Temmerman, J. Senden, B. Buis, Continuous measurement of left ventricular volume in animals and humans by conductance catheter, Circulation 70 (1984) 812.
[16] D. Burkhoff, E. van der Velde, D. Kass, J. Baan, W.L. Maughan, K. Sagawa, Accuracy of volume measurement by conductance catheter in isolated, ejecting canine hearts, Circulation 72 (2) (1985) 440.
[17] B. Lambermont, P. Kolh, A. Ghuysen, P. Segers, J.-M. Dogn, V. Tchana-Sato, P. Morimont, P. Benoit, P. Grard, B. Masereel, V. D'Orio, Effect of a novel thromboxane a2 inhibitor on right ventricular-arterial coupling in endotoxic shock, Shock 21 (1) (2004) 45.
[18] V. D'Orio, B. Lambermont, O. Detry, P. Kolh, P. Potty, P. Gerard, R. Marcelle, Pulmonary impedance and right ventricular-vascular coupling in endotoxin shock, Cardiovasc. Res. 38 (2) (1998) 375.
[19] A. Kimchi, A.G. Ellrodt, D.S. Berman, M.S. Riedinger, H.J. Swan, G.H. Murata, Right ventricular performance in septic shock: a combined radionuclide and hemodynamic study, J. Am. Coll. Cardiol. 4 (5) (1984) 945.
[20] A.J. Schneider, G.J. Teule, A.D. Kester, G.A. Heidendal, L.G. Thijs, Biventricular function during volume loading in porcine *E. coli* septic shock, with emphasis on right ventricular function, Circ. Shock 18 (1) (1986) 53.
[21] G.J. Teule, A. van Lingen, A.J. Schneider, M.A. Verwey van Vught, A.D. Kester, G.A. Heidendal, L.G. Thijs, Left and right ventricular function in porcine *Escherichia coli* sepsis, Circ. Shock 15 (3) (1985) 185.